Increased risk of groundwater contamination due to saltwater intrusion driven by climate change in Casco Bay, Maine

Matthew Guiang[1], Melissa R. Allen[1]

[1]Oak Ridge National Laboratory

Abstract. Changing precipitation patterns resulting from climate change are likely to affect the future availability of freshwater resources. Coastal aquifers are especially vulnerable to such changes in the form of contamination via the intrusion of saltwater as sea level rises. In Casco Bay, Maine, the population depends largely on groundwater from private wells as a source of freshwater. Thus, assessing the vulnerabilities of coastal and island aquifers to saltwater intrusion influenced by climate change is important. This study examines the aggregate effects of sea level rise, changing precipitation patterns, and population shifts (well pumping rate) on the depth of the freshwater-saltwater interface. Well vulnerability to these changes is determined by comparison of average well depth to the resulting interface depth. Although vulnerabilities of individual wells are difficult to predict given that hydraulic properties are governed by complex fracture patterns, this preliminary model demonstrates a representative response of bedrock aquifers of Casco Bay to climate and population stresses. We find that changing precipitation patterns have the greatest effect on interface depth variations, exceeding those caused by sea level rise. Wells near shore where the interface is the shallowest are particularly vulnerable to contamination by saltwater intrusion and should be considered vulnerable even under best-case conditions. In multiple climate change scenarios, the saltwater-freshwater interface decreases in depth, indicating greater vulnerability to contamination over time for populations reliant on groundwater from bedrock aquifer wells.

1.0 Introduction

The changing climate has cast into focus the importance of the future availability of freshwater resources (Ferguson and Gleeson, 2012; Milly et al., 2005; Vorosmarty et al., 2000). Fluctuating regional populations, coupled with changing weather patterns, alter demand and supply limiting the availability future freshwater resources. In areas such as coastal Maine, where the population is largely dependent upon groundwater extracted from fractured, confined bedrock aquifers, changing precipitation patterns are expected to have significant impacts on the amounts of subsurface freshwater (Caswell, 1979). Specifically, sea level rise will alter aquifer hydraulic gradients. Changing rates of precipitation will result in changing rates of aquifer recharge, which will in turn have an effect on the flow of groundwater through aquifer systems. In the area of Casco Bay, Maine (Figure 1), where island and peninsular wells are predominantly drilled into confined bedrock aquifers, these changes become especially important due to networks of fractures that serve as conduits for both freshwater and saltwater to flow into and out of the aquifer. Changes in flow patterns due to rising sea levels and changing rates of recharge can result in the inward flow of saltwater from the sea into the aquifer, effectively contaminating the freshwater resource.

Saltwater intrusion poses a great risk to the residents of coastal Maine due to its relative permanence and difficulty to reverse, especially for communities in which aquifers provide the sole source of drinking water (Tuttle, 2007). Coastal areas analogous to Casco Bay have been observed to experience intrusion (Caswell, 1979; Tuttle, 2007) and are likely to become more vulnerable due to the effects related to climate change. A preliminary analysis of saltwater intrusion risk from sea level rise in Casco Bay, Maine finds that the hydraulic gradient weakens with sea level rise to the point of becoming negative, at which point saltwater flows inward and contaminates the aquifer, demonstrating the vulnerability of these coastal aquifers to saltwater intrusion due to sea level rise. This further analysis uses the United States Geology Survey MODFLOW-2005 program (Harbaugh, 2005) to simulate groundwater flow for an example Casco Bay bedrock aquifer and to assess the likelihood of saltwater intrusion of wells under three different influences: 1) sea level rise 2) changing rates of aquifer recharge under the worst case (8.5 W m^{-2} radiative forcing by 2011) Representative Concentration Pathway Scenario (RCP 8.5) precipitation projections, and 3) changing pumping rates due to population shifts.

2.0 Background

2.1 Confined Bedrock Aquifers

Approximately 40% of Maine's population depends on groundwater for residential use (Caswell, 1979). Residents of the islands and peninsulas in Casco Bay rely predominantly on groundwater supplied by wells drilled into fractured, confined bedrock aquifers, the characteristics of which are significant factors affecting the subsurface flow. A map of the private confined bedrock aquifer wells in the Casco Bay area can be seen in Figure 2. A confined aquifer is defined as bedrock overlain by thick permeable soils or pervious bedrock with no soil that is fully saturated with water under pressure (Bobba, 1993). Confined bedrock aquifers exist only where rock is fractured and capable of holding water. Flow of groundwater in such aquifers is slow, and its recharge occurs through regular precipitation.

Freshwater in coastal aquifers such as those in Casco Bay, where islands and peninsulas are surrounded by saltwater, exists as a lens that floats above the saltwater in isostatic equilibrium, a schematic of which is shown in Figure 3 (modified from Caswell, 1979). The depth of the saltwater-freshwater interface varies seasonally and depends upon climatic conditions, flow within the system, and the extent of groundwater extraction, and is related to the height of the water table elevation by the density ratio of freshwater to saltwater, given by the Ghyben-Herzberg approximation (Herzberg, 1901; Ghyben, 1888):

(1)

where $z = z(x)$ is the depth of the freshwater-saltwater interface below mean sea level, is the fresh water density, is the saltwater density, and $h = h(x)$ is the water table elevation above mean sea level (Werner and Simmons, 2009). This ratio is generally considered to be 40:1, meaning that for every foot of freshwater in the aquifer above sea level the lens extends 40 feet below sea level. Correspondingly, for every foot of water drawdown caused by pumping, there is an upwelling of the saltwater-freshwater interface of 40 feet. Due to this relationship, Ferguson and

Gleeson (2012) find that such coastal aquifers are more vulnerable to saltwater intrusion due to groundwater extraction than to predicted sea level rise.

Saltwater intrusion into coastal bedrock aquifers occurs where significant freshwater-bearing fractures, typically associated with faults, intersect large fractures that cut across the land and extend to the ocean (Caswell, 1987). These fractures provide saltwater with a path to reach the freshwater stored in bedrock aquifers. Under the conditions of a negative hydraulic gradient, saltwater flows inward from the ocean through these fractures resulting in the migration of the freshwater-saltwater boundary inwards and the consequent contamination of bedrock aquifer wells. It has been shown by Masterson (2004) that for Cape Cod aquifers from years 1921 to 2000, the hydraulic gradient weakens with sea level rise, assuming the water table elevation does not change. In the generalized case study of Werner and Simmons (2009), a similar result was found for head-controlled aquifer systems.

2.2 Geologic Setting

Bedrock in the Harpswell area of Casco Bay consists primarily of metamorphic stratified schistose and granofelsic rocks, predominantly from two geologic formations: the Sebascodegan formation, a thin-bedded quartz-plagioclase-biotite granofels and gneiss, and the Cape Elizabeth formation, a thin-bedded siliceous and sericitic slate with beds of greywacke slate and schist (Hussey, 1985; Hussey and Marvinney, 2002). These geologic units were heavily deformed and metamorphosed at great depths and pressures during the continental collision that formed the Appalachians, resulting in extensive regional faulting and folding, which contributes greatly to the presence of fractures that control groundwater flow in coastal aquifers. Two major oppositely striking thrust faults of moderate dip (~80°) run roughly N-S through Sebascodegan Island, and are coincident with major topographic features and foliation, and are likely related to many of the water bearing fractures in the area (Hussey, 1985; Caswell, 1979). Sand, gravel, and unconsolidated sediments of varying thickness deposited during the last glacial period cover much of Casco Bay. On Sebascodegan Island the surficial materials are predominantly less than three feet of glacial drift covering bedrock or a thin deposit of poorly sorted till.

3.0 Methods

In order to quantify the effect of sea level rise on the vulnerability of Casco Bay's island bedrock wells to saltwater intrusion, we configured a model of groundwater flow for a hypothetical representative island aquifer using the modular finite-difference groundwater flow model (MODFLOW) developed by the United States Geological Survey (USGS; McDonald and Harbaugh, 1988). This model is the most widely used in the world for simulating groundwater flow and has been validated extensively since its publication in 1988 (USGS, 1997). MODFLOW-2005 models the three-dimensional flow of groundwater of constant density through porous material based on the partial differential equation (Harbaugh, 2005)

(2)

where K_{xx}, K_{yy}, and K_{zz} are the hydraulic conductivities in the x, y, and z, directions; h is the potentiometric head; W is the volumetric flux per unit volume, S_s is the specific storage of the material; and t is time. MODFLOW-2005 uses the finite-difference method to obtain approximate analytical solutions to obtain time-varying head distributions that can be used to characterize the flow system and to calculate the direction and rate of groundwater flow.

The SWI2 package (Bakker et al., 2013) for MODFLOW was added to simulate seawater intrusion into the aquifer allowing for three-dimensional vertically integrated variable-density groundwater flow analysis. The SWI2 package models variable-density flow in an isotropic aquifer, based on Darcy's law for variable-density flow, which can be written as (Post et al., 2007; Bakker et al., 2013)

(3)

where q_x, q_y, and q_z are the specific discharge components in the x, y, and z directions; K is the freshwater hydraulic conductivity; h_f is the freshwater head, and v is the dimensionless density. The SWI2 package allows for the effects of density differences to be incorporated into MODFLOW-2005, and uses the Dupuit approximation in which an aquifer is vertically discretized into zones of differing densities. Derivations of Equations 1 and 2 can be found in Rushton and Redshaw (1979) and Bakker et al. (2013), respectively. This model does not consider variations in viscosity and the effects of dispersion and diffusion. The user interface, ModelMuse Version 3, (Winston, 2014) was used as a pre-and post-processing tool for our simulation.

We represent Casco Bay aquifers in MODFLOW using a representative island, Sebascodegan Island. The island includes a specified flux boundary to which a recharge rate is applied. The island aquifer is surrounded by ocean extending offshore along all sides that is represented in MODFLOW by a General Head Boundary (GHB) condition in model layer 1 with an altitude set to the current sea level, after Bjerklie et al. (2012). To simulate gradual sea level rise, constant heads are increased at yearly intervals at the rate of projected sea level rise.

The model domain is discretized into a finite-difference grid of 101 columns and 120 rows, with cell sizes measuring 75 by 100 m. The upper surface of the model corresponds to the surface elevation provided by elevation contours of Sebascodegan Island. The hypothetical aquifer consists of two layers: a thin unit of unconsolidated gravelly glacial drift overlaying a confined layer of fractured crystalline bedrock that extends to 400 m below sea level. The bottom of the model is defined as a no flow boundary.

Our instance of the model was designed to simulate the effects of sea level rise on the island's coastal aquifer for the years 2000-2070, incorporating the effects of changing precipitation and recharge rates, as well changing pumping rates associated with population changes. After establishing a steady-state condition, the model was used to simulate hypothetical scenarios of long-term change in sea level and aquifer recharge under Representative Concentration Pathway

8.5 (RCP 8.5), the worst case scenario achieving a climate forcing of 8.5 W m^{-2} by 2100. Two sea level rise scenarios were also considered, which assumed a global sea level rise of 1 m and 2 m, respectively, over the next century.

A total of 270 years was simulated, using one preliminary stress period of 200 years to establish current, steady-state aquifer conditions, and the following 70 years to simulate aquifer development under projected changes in sea level and recharge. Storage changes between aquifers were not considered, and all stress periods are steady-state.

3.1. Data Sets

Geologic, hydrologic, climactic, and population data are based on observations and projections for Sebascodegan Island and are presumed to be representative of regional island aquifer conditions. The following data sets are used as those inputs to the model.

3.1.1. Sea Level Rise

Sea level rise estimates are based on those of the National Oceanic and Atmospheric Administration for the United States National Climate Assessment (NCA, 2014), which indicate a "greater than 90% chance" that global mean sea level will rise at least 0.2 meter and no more than 2.0 meters by 2100.

3.1.2. Precipitation and Recharge

Precipitation data (Appendix Figure 2) used to calculate aquifer rate of recharge (Figure 4) are cumulative monthly values at 4 km resolution from the Weather Research and Forecasting (WRF) model dynamically downscaled from Community Earth System Model, Version 1.0 (CESM1) projections at 1 x 1.25 degree spatial resolution under RCP 8.5. The CESM simulation, output at 3-hourly intervals, is an ensemble member of the Coupled Model Intercomparison Project, Version 5 (CIMP5) (Gao et al., 2012). Recharge is calculated as 7.95% of precipitation (Gerber and Hebson, 1996). Base-case and 2050 recharge rates were calculated for our simulation, and intermediate years were interpolated from these data.

3.1.3. LandScan Population Projections and Pumping Rates

The LandScan and LandCast data sets at 1 km resolution were created using a multi-variable dasymetric modeling approach along with spatial data and imagery analysis technologies to disaggregate census counts within administrative boundaries at the town, county, and state levels (http://web.ornl.gov/sci/landscan/ landscan_documentation.shtml). LandCast 2050 population projections (McKee et al., 2015) incorporate the cohort-component methodology outlined by the U.S. Census along with urbanization/land cover conversion projections. Population from these data sets is then aggregated to the census tract (Appendix Figure 1) to provide proxy communities supplied by individual private wells.

Pumping rates were calculated based on a 51 gallons per capita day (gpcd) estimate of Maine public water usage presented by Kenny et al. (2009) and multiplied by projected populations for Sebascodegan Island for 2004 and 2050. Since the vast majority of pumping in the region is from private bedrock wells (Caswell, 1979), this is an appropriate estimate. Wells were simulated using the WEL package in MODFLOW, pumping at a depth of 60 m, an average depth of bedrock wells in the region (Caswell, 1979; Loiselle and Evans, 1995).

3.1.4. Hydraulic Properties and Boundary Conditions

Aquifer properties, (Supplementary Materials Table 1), were assigned based on previously measured data and generalized surficial and bedrock geology of the Casco Bay area. The unit comprising layer 1 is separated into two units (Supplementary Materials Figure 3B): fine-grained glaciomoraine deposits (Presumpscot Formation) and glacial till. Surficial materials have various thicknesses interpolated from the overburden thickness of island wells. Horizontal hydraulic conductivity for the Presumpscot Formation and glacial till is 0.00189 and 1.122 m/d, respectively (Brainerd et al., 1996; Morrissey (1983). Vertical Hydraulic conductivity of the Presumpscot Formation is $8.23*10^{-6}$ m/d (Nielsen et al., 1995).

Model layer 2 represents heterogeneous anisotropic crystalline fractured metamorphic bedrock where hydraulic conductivity can vary over at least six orders of magnitude (Johnson, 1999). However, Shapiro (2002) shows that at large enough scales, bulk bedrock aquifer properties may be used to infer regional distributions of groundwater. While complex fracture networks govern hydraulic conductivity at small scales, on scales larger than 100 m the effective hydraulic conductivity of the bedrock is more strongly controlled by the larger fracture network and bulk hydraulic properties. Furthermore, Loiselle and Evans (1995) find that in the region of study, fracture permeability remains uniform with depth, validating the use of bulk hydraulic properties for a large-scale model. Thus, layer 2 is modeled as a homogeneous isotropic layer with a hydraulic conductivity of 0.277 m/d, based on a range of estimates made by Johnson (1999) on similar fractured bedrock. No hydrogeological data was available for the specific bedrock units considered in this study.

As a result of these generalizations, this model must be considered preliminary and requires further, site-specific hydrogeological studies to better constrain the findings of this study. Further, the complex nature and spatial heterogeneity of hydraulic properties of fractured bedrock aquifers limits the ability of this model to predict vulnerability of wells on an individual scale. Rather, this model serves primarily to predict aquifer lens depth at a larger scale and its response to changes relating to climate and population shifts.

4.0 Results and Discussion

Ten scenarios, shown in Table 1, were simulated using the model. These included a “best” and “worst” case scenario, in order to demonstrate the potential range of responses for the aquifer. The simplest three scenarios demonstrate the individual effects of 0 m, 1 m, and 2 m sea level rise with pumping and recharge rates held constant. An additional three scenarios incorporate projected changes in recharge and pumping rates with the assumed 0 m, 1 m, and 2 m sea level rise. The final two scenarios consider high and low rates of recharge, with sea level constant at 0 m and pumping absent. After each simulation, the depth of the saltwater-freshwater interface was compared to the average well depth (60 m) to determine saltwater contamination vulnerability. Where the interface depth is shallower than the average well depth, we consider that well location vulnerable to saltwater intrusion.

Figure 5 shows the depths of the saltwater-freshwater interface for a cross section of the island under multiple scenarios. In a best case scenario (Figure 5B) assuming no sea level rise, highest-possible recharge rate, and lowest-possible pumping rate, the depth of the interface is up to 21 m deeper than the worst case scenario that assumes 2 m sea level rise by 2100, lowest possible recharge rate, and highest possible pumping rate. Figure 5C shows the projected interface depths for a cross section of the island based on projected changes in recharge and pumping rates under three possible sea level rise scenarios (0 m, 1 m, and 2 m by 2100). The effect of sea level rise can be seen as the depth of the lens decreases by as much as 14 m between 0 m and 2 m sea level rise scenarios.

In scenarios 3-4 and 8-10, which examine the individual effects of sea level rise and recharge, respectively, we find that recharge rate has a more significant effect on interface depth than that of projected sea level rise. Also, while pumping does have an effect on the depth of the interface, the rate of pumping occurring at private wells is only enough to cause minor upwellings in the interface. Such an upwelling can be seen in Figure 5C. Thus, over-pumping at private wells is not likely to be a leading contributor to saltwater intrusion, compared to other coastal regions where over-pumping from groundwater wells is the primary cause of saltwater intrusion (Barlow and Reichard, 2010).

To determine the vulnerability of individual wells given changes in the saltwater-freshwater interface of the model Sebascodegan Island, geospatially located model wells (Figure 6) of representative depth were used in the simulation. In the best case scenario (Figure 6A), 13 of the 168 total model wells were below the saltwater-freshwater interface (contaminated), assuming an average well depth of 60 m. In the worst case scenario (Figure 6B), the number of contaminated wells was 19. In the climate projection assuming 0 m sea level rise (Figure 6C), 14 wells were contaminated. In the climate projection assuming 2 m sea level rise (Figure 6D), 15 wells were contaminated.

We find that wells close to shore, where the interface is shallowest, are particularly vulnerable to contamination by saltwater intrusion and should be considered vulnerable even under best-case conditions. With increasingly severe climate change scenarios, the overall depth of the interface decreases, increasing the likelihood of saltwater intrusion into wells. In possible climate change scenarios 5-7 the saltwater-freshwater interface decreases in depth, indicating increased vulnerability to contamination over time for populations reliant on groundwater from bedrock wells. Although individual well vulnerability is difficult to predict given hydraulic properties are governed by complex fracture patterns, this preliminary model is useful in demonstrating the response of bedrock aquifers to climate and population stresses.

It must be stressed that results of this preliminary model demonstrate the only the generalized qualitative response of a coastal bedrock aquifer in Casco Bay to population shifts and the precipitation and sea level changes accompanying climate change. The heterogeneous and complex nature of the bedrock in question can contribute to hydraulic properties varying over many orders of magnitude, variations that can significantly impact models of this kind. In order to better constrain modeling parameters and thus gain more detailed information regarding the vulnerability of specific aquifers, site-specific hydrogeologic data is needed for the bedrock and surficial materials in the region. Improving and localizing estimates of hydraulic properties will serve to paint a more accurate picture of the vulnerability of these aquifers.

5.0 Conclusions

We find that climate change projections indicate increased annual precipitation (although mostly in the form of larger extreme events) for the islands in the Casco Bay area. Coupled with a projected decrease in population, and therefore a decrease in private pumping rates, this change seems unlikely to put freshwater wells drawing from confined bedrock aquifers at risk. However, the effects of sea level rise could serve to decrease the depth of the interface to the point at which risk is increased for some wells. Thus, although mitigated by a projected increase in precipitation amounts for the northeast, a rise in sea level causes significant shallowing of the saltwater-freshwater interface, and the sum total of the effects climate change could contribute to the possible contamination of some private wells. While individual well vulnerability is difficult to predict given the complex and heterogeneous nature of fractured bedrock, deep wells that are close to shore are most at risk for contamination, and should be considered especially vulnerable to this long term consequence of climate change.

6.0 Acknowledgements

This manuscript has been authored by employees of UT-Battelle, LLC, under contract DE-AC05-00OR22725 with the U.S. Department of Energy. Accordingly, the publisher, by accepting the article for publication, acknowledges that the United States Government retains a nonexclusive, paid-up, irrevocable, world-wide license to publish or reproduce the published form of this manuscript, or allow others to do so, for United States Government purposes.

The authors would like to acknowledge the financial support for this research from the United States Department of Homeland Security (DHS) Regional Resiliency Assessment Program (RRAP) and from the U. S. Department of Energy Office of Science (DOESC) and the Oak Ridge Institute for Science and Education (ORISE) Science Undergraduate Laboratory Internships (SULI) at Oak Ridge National Laboratory. We also gratefully acknowledge the intellectual and data contributions of DHS's Donald Kim Erskine, IP Regional Director, Federal Region 1 and William Delong, PSA Maine District; Duane Verner, Risk and Infrastructure Science Center (RISC), Global Security Sciences Division, Argonne National Laboratory; Robert Marvinney, Maine State Geologist; and Steven Fernandez, Civil and Environmental Engineering, University of Tennessee. We thank Scott Painter, Subsurface Flow and Reactive Transport Modeling, Oak Ridge National Laboratory, for his very helpful internal review comments.

References

Bakker, M., Schaars, F., Hughes, J.D., Langevin, C.D., and Dausman, A.M.: Documentation of the seawater intrusion (SWI2) package for MODFLOW, U.S. Geological Survey Techniques and Methods, book 6, chap. A46, 47 p., 2013.

Barlow, P. M. and Reichard, E. G.: Saltwater intrusion in coastal regions of North America, Hydrogeology Journal, 18, 247-260, 2010.

Bjerklie, D. M., Mullaney, J. R., Stone, J. R., Skinner, B. J., and Ramlow, M. A.: Preliminary investigation of the effects of sea-level rise on groundwater levels in New Haven, Connecticut, U.S. Geological Survey Open-File Report 2012-1025, 46 p., 2012.

Bobba, A. G.: Mathematical model for saltwater intrusion in coastal aquifers, Water Resources Management, 7, 3-37, 1993.

Brainerd, E. C., Hebson, C. S., and Gerber, R. G.: Hydrogeology of Presumpscot clay-silt using isotopes, in Loiselle, M., Weddle, T. K., and White, C.: Selected papers on the hydrogeology of Maine: Geological Society of Maine, Bulletin 4, Augusta, Maine, 81-94, 1996.

Caswell, W. B.: Maine's ground-water situation, Ground Water, 17, 235-243, 1979.

Caswell, W. B.: Ground water handbook for the state of Maine, Maine Geological Survey, Bulletin 39, 1-135, 1987.

Ferguson, G. and Gleeson, T.: Vulnerability of coastal aquifers to groundwater use and climate change, Nature Climate Change, 2, 342-345, 2012.

Gao, Y., Fu, J. S., Drake, J. B., Liu, Y., and Lamarque, J. F.: Projected changes of extreme weather events in the eastern United States based on a high resolution climate modeling system, Environ Res Lett, 7, 044025, 2012.

Gerber, R. G. and Hebson, C. S.: Bulletin4: Selected Papers on the Hydrogeology of Maine, Geological Society of Maine, 30p, 1996.

Ghyben, B. W.: Nota in Verband met de Voorgenomen Putboring Nabij Amsterdam, Amsterdam, Tijdschr. Kon. Inst. Ing., 9, 8–22, 1888.

Harbaugh, A.W., MODFLOW-2005, The U.S. Geological Survey modular ground-water model -- the Ground-Water Flow Process: U.S. Geological Survey Techniques and Methods 6-A16, 253 p., 2005.

Herzberg, A.: Die Wasserversorgung einiger Nordseebäder, J. Gasbeleucht. Wasserversorg., 44, 815–819, 842–844, 1901.

Hussey, A.M., II: The bedrock geology of the Bath and Portland 2° map sheets, Maine, Maine Geological Survey, Open-File No. 85-87, 88 p., 1985.

Hussey, A. M., II, and Marvinney, R. G.: Bedrock geology of the Bath 1:100,000 quadrangle, Maine Geological Survey, Geologic Map 02-152, color map, cross section, scale 1:100,000, 2002.

Johnson, C. D.: Effects of lithology and fracture characteristics on hydraulic properties in crystalline rock: Mirror Lake Research Site, Grafton County, New Hampshire, in Morganwalp, D. W. and Buxton, H. T., eds., U.S. Geological Survey Toxic Substances Hydrology Program-Proceedings of the Technical Meeting, Charleston, South Carolina, March 8-12, 1999, U.S. Geological Survey Water-Resources Investigation Report 99- 4018C, v. 3, p. 795-802, 1999.

Kenny, J. F., Barber, N. L., Hutson, S. S., Linsey, K. S., Lovelace, J. K., and Maupin, M. A.: Estimated use of water in the United States in 2005, U. S. Geological Survey Circular 1344, 52 p., 2009.

Loiselle, M. and Evans, D.: Fracture density distributions and well yields in Coastal Maine, Ground Water, 33/2, 190-196, 1995.

Lombard, P. J.: Maine StreamStats: a water-resources web application, U. S. Geological Survey, Fact Sheet 2015-3014, 2015.

Maine Office of Geographic Information Systems Data Catalog, Downloaded June, 2015, http://www.maine.gov/megis/catalog/

Masterson, J. P.: Simulated interaction between freshwater and saltwater and effects of groundwater pumping and sea-level change, Lower Cape Cod aquifer system, Massachusetts, USGS Scientific Investigations report, 2004-5014, 78 p., 2004.

McDonald, M.G. and Harbaugh, A.W., A modular three-dimensional finite-difference ground-water flow model: Techniques of Water-Resources Investigations of the United States Geological Survey, Book 6, Chapter A1, 586 p, 1998.

McKee, J. J., Rose, A. N., Bright, E., Huynh, T., and Bhaduri, B.: A locally-adaptive, spatially-explicit projection of U.S. Population for 2030 and 2050, Proceedings of the National Academy of Sciences, 112/5, 1344-1349, 2015.

Milly, P. C. D., Dunne, K. A. and Vecchia, A. V.: Global pattern of trends in streamflow and water availability in a changing climate, Nature, 438, 347–350, 2005.

Morrissey, D. J.: Hydrology of the Little Androscoggin River Valley Aquifer, Oxford County, Maine, U. S. Geological Survey Water-Resources Investigations, 83-4018, 87 p., 1983.

NCA Climate Change Impacts in the United States, U.S. National Climate Assessment (Washington, DC: U.S. Global Change Research Program, 2014).

Nielsen, M. G., Stone, J. R., Hansen, B. P., and Nielsen, J. P.: Geohydrology, water quality, and conceptual model of the hydrologic system, Saco Landfill, area, Saco, Maine, U. S. Geological Survey Water-Resources Investigations Report 95-4027, 95 p., 1995.

Post, V. Kooi, H., and Simmons, C.: Using hydraulic head measurements in variable –density ground water flow analyses, Groundwater, 46/6, 664-671, 2007.

Rushton, K. R. and Redshaw, S. C.: Seepage and groundwater flow: numerical analysis by analog and digital methods, Wiley, 1979.

Shapiro, A. M.: Characterizing fractured rock for water supply: From well field to the water-shed, Fractured-Rock Aquifers, Proceeding National Ground Water Association, Denver, Colorado, 6-9, 2002

Tolman, S. S. (compiler): Bedrock well depths in the Bath 30x60-minute quadrangle, Maine, Maine Geological Survey, Open-File Map 10-34, map, scale 1:125,000, 2010b.

Tolman, S. S. (compiler): Overburden thickness in the Bath 30x60-minute quadrangle, Maine, Maine Geological Survey, Open-File Map 10-35, map, scale 1:125,000, 2010a.

Tuttle, S.: Water Resources of Part of the West Coast of Vinalhaven Island, Penobscot Bay, Maine, Bachelor's Honors Thesis, 2007.

U. S. Geological Survey, Modeling ground-water flow with MODFLOW and related programs, U. S. Geological Survey, Fact Sheet 121-97, 1997.

Vorosmarty, C. J., Green, P., Salisbury, J. and Lammers, R. B.: Global water resources: Vulnerability from climate change and population growth, Science, 289, 284–288, 2000.

Werner, A. D. and Simmons, C. T.: Impact of Sea Level Rise on Sea Water Intrusion in Coastal Aquifers, Ground Water, 47/2, 197-204, 2009.

Winston, R.B.: ModelMuse - A graphical user interface for MODFLOW–2005 and PHAST: U.S. Geological Survey Techniques and Methods 6–A29, 52 p., 2009.

Figures

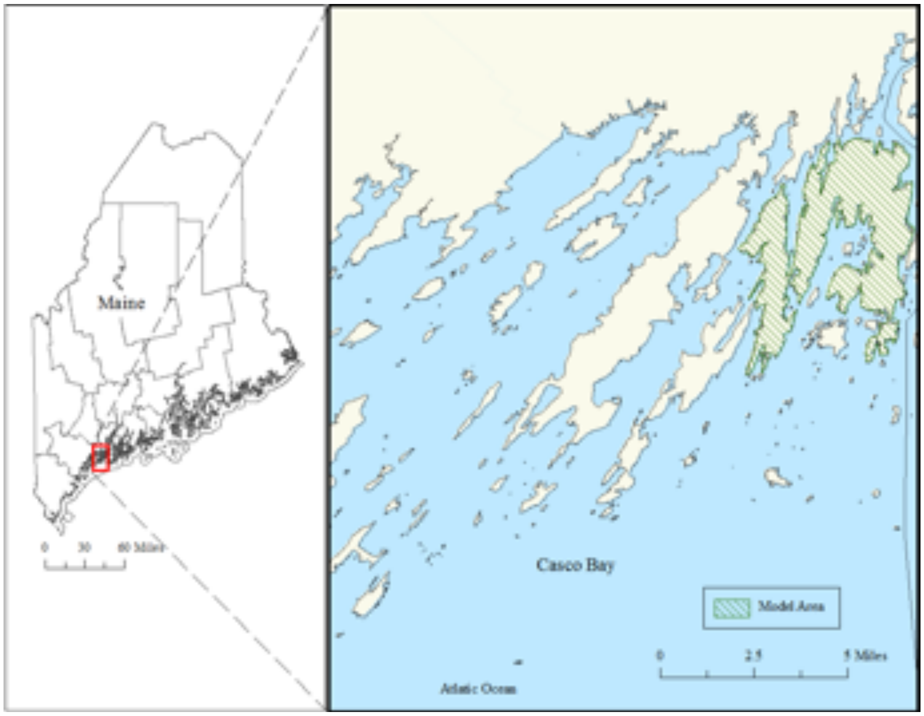

Figure 1. Map showing region of study with model area represented by the shaded region (image modified from the Maine Office of GIS).

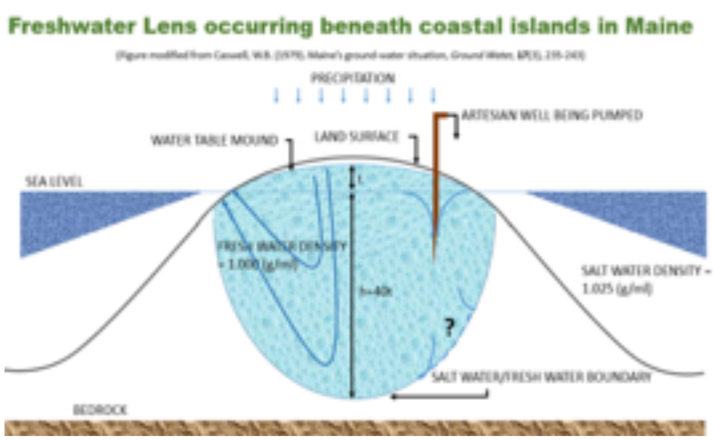

Figure 3. Schematic showing the idealized geometry of the freshwater lens which floats above the surrounding salt water. The depth of the lens (h) is based on saltwater-freshwater density ratio and approximately equal to 40t (image modified from Caswell, 1979).

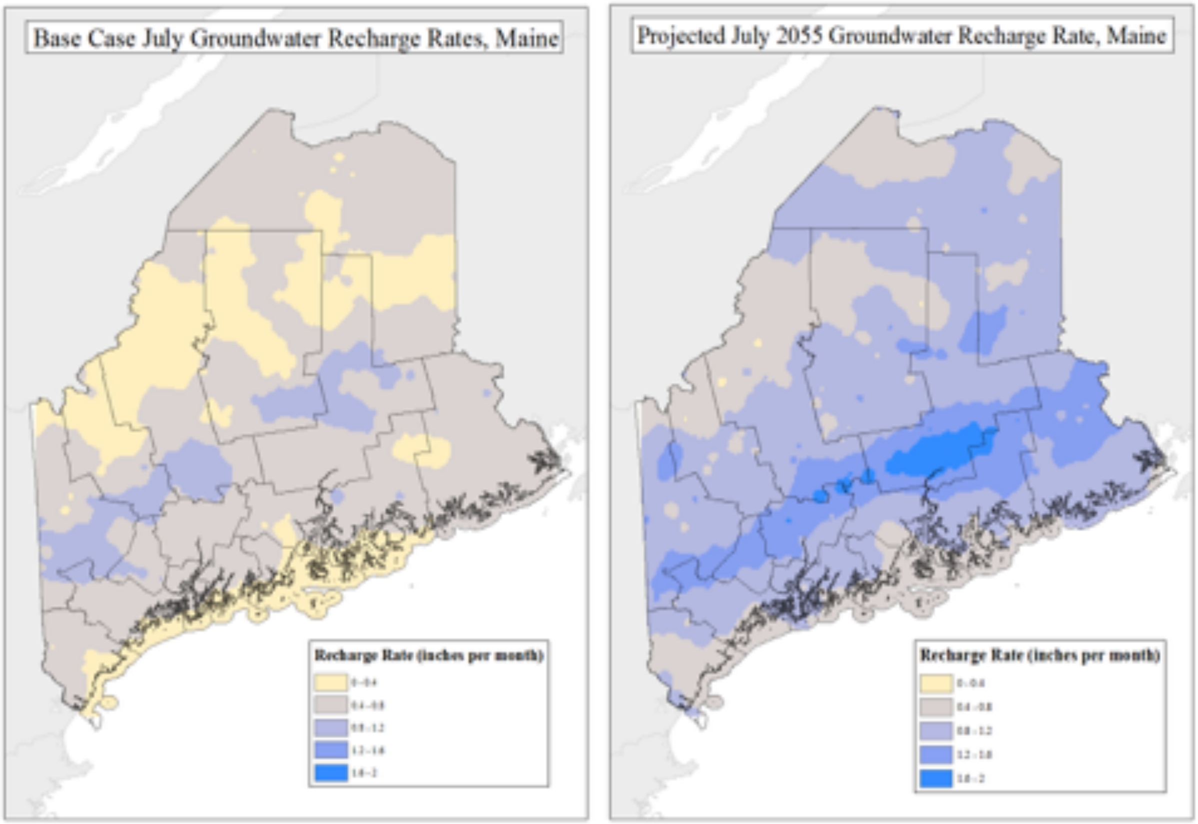

Figure 4. Map showing July projected base-case and 2055 recharge rates. Recharge rates are calculated as 7.95% of precipitation (projected using WRF dynamically downscaled data) (Gerber and Hebson, 1996). Base-case and 2050 recharge rates were calculated for our simulation, and intermediate years were interpolated from these data.

Figure 5. (A) Map of model area showing cross section A-A’. (B) Plot of saltwater-freshwater interface depth (m) for a best case scenario (green) assuming no sea level rise, highest-possible recharge rate, and lowest-possible pumping rate, and worst case scenario (orange) that assumes 2 m sea level rise by 2100, lowest-possible recharge rate, and highest-possible pumping rate. The depth of the worst case interface is up to 21 m shallower than the best case interface. (C) Plot of saltwater-freshwater interface depth for climate change projection scenarios considering 0 m (red), 1 m (green) and 2 m (blue) sea level rise. The depth of the interface can be seen to be decreasing by as much as 14 m under increased sea level rise.

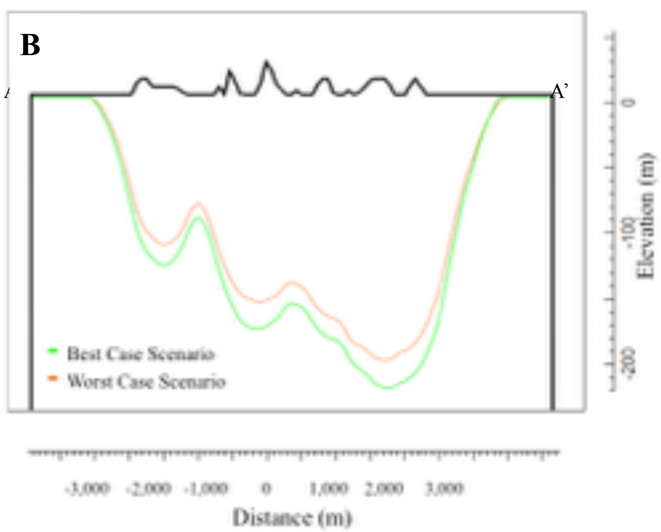

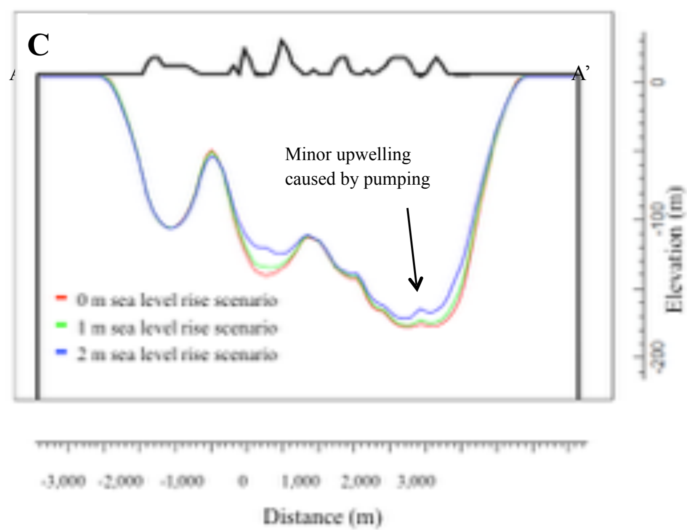

Figure 6. Map showing model wells and contaminated wells in 2070 assuming an average well depth of 60 m, based on (A) best case, (B) worst case, (C) 0 m sea level rise, and (D) 2 m sea level rise scenarios. In the best case scenario (A), 13 of the total 168 model wells is below the saltwater-freshwater interface (contaminated). In the worst case scenario (B), the number of contaminated wells is 19. In the climate projection assuming 0 m sea level rise (C), 14 wells are contaminated. In the climate projection assuming 2 m sea level rise (D), 15 wells are contaminated.

Table 1. Model Scenarios

	Scenario	Sea Level Start (m)	Sea Level End (m)	Recharge Start (m/d)	Recharge Start (m/d)	Pumping Rate Start (m^3/d)	Pumping Rate End (m^3/d)
1	Worst Case	2	2	0.000282795	0.000282795	-3.175	-3.175
2	Best Case	0	0	0.000356452	0.000356452	-2.75	-2.75
3	High Recharge	0	0	0.000282795	0.000282785	0	0
4	Low Recharge	0	0	0.000356452	0.000356452	0	0
5	Projection 1 (2 m sea level rise)	0	2	0.000282795	0.000356452	-3.175	-2.75
6	Projection 2 (1 m sea level rise)	0	1	0.000282795	0.000356452	-3.175	-2.75
7	Projection 3 (0 m sea level rise)	0	0	0.000282795	0.000356452	-3.175	-2.75
8	0 m Sea Level Rise	0	0	0.000282795	0.000282795	-3.175	-3.175
9	1 m Sea Level Rise	0	1	0.000282795	0.000282795	-3.175	-3.175
10	2 m Sea Level Rise	0	2	0.000282795	0.000282795	-3.175	-3.175

Supplementary Material

Table 1. Hydraulic Properties of Aquifer Materials

Geologic Material	Layer	Horizontal Hydraulic Conductivity (K_x, m/day)	Vertical Hydraulic Conductivity (K_z, m/day)	Source
Fine-grained glaciomoraine deposits (Presumpscot Formation)	1	0.001889	$8.23*10^{-6*}$	Brainerd et al., 1996 ;*Nielsen et al., 1995
Till	1	1.121	1.21	Morrissey, 1983
Fractured Metamorphic Crystalline Bedrock	2	0.277	0.277	Johnson, 1999

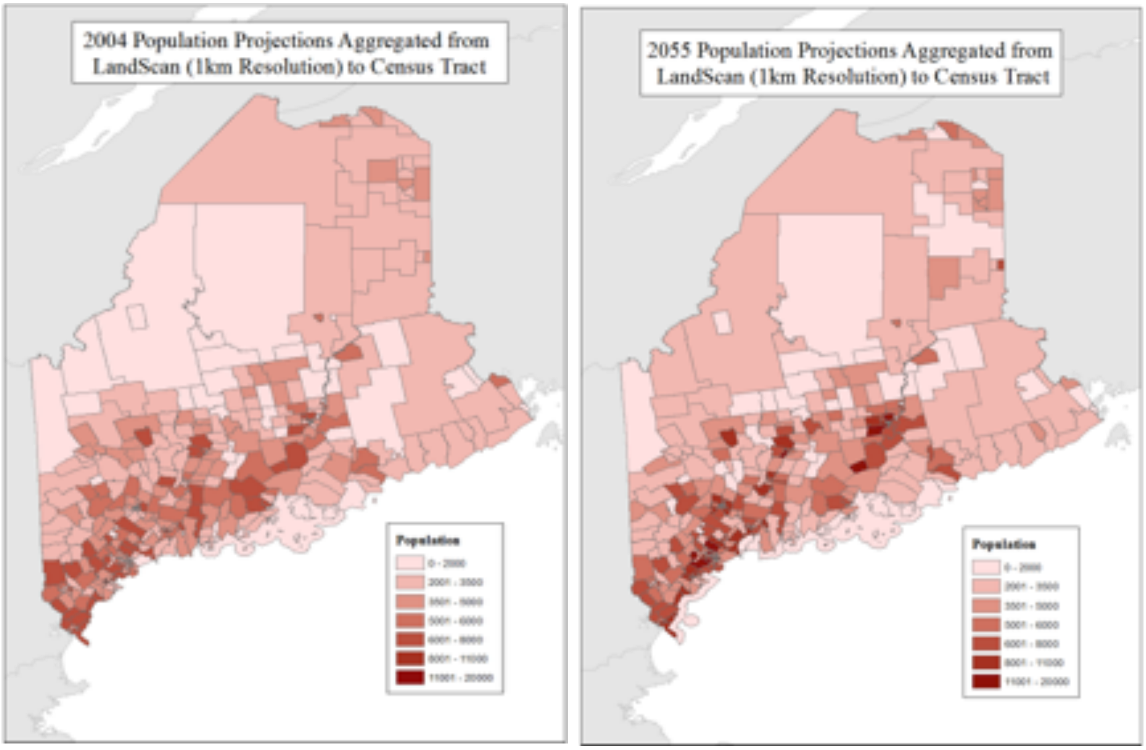

Figure 1. 2004 (base case) and 2055 population projections aggregated from LandScan (1 km resolution) to census tract. Population projections for Sebascodegan Island for 2004 are 2,763 and 1,893, respectively. Multiplying these populations by the gallons per capita day (gpcd) private well water use estimates provided by Kenny et al. (2009) gives the total pumping rate per day.

Figure 2. July projected base case and 2055 precipitation rates, based on WRF downscaled data.

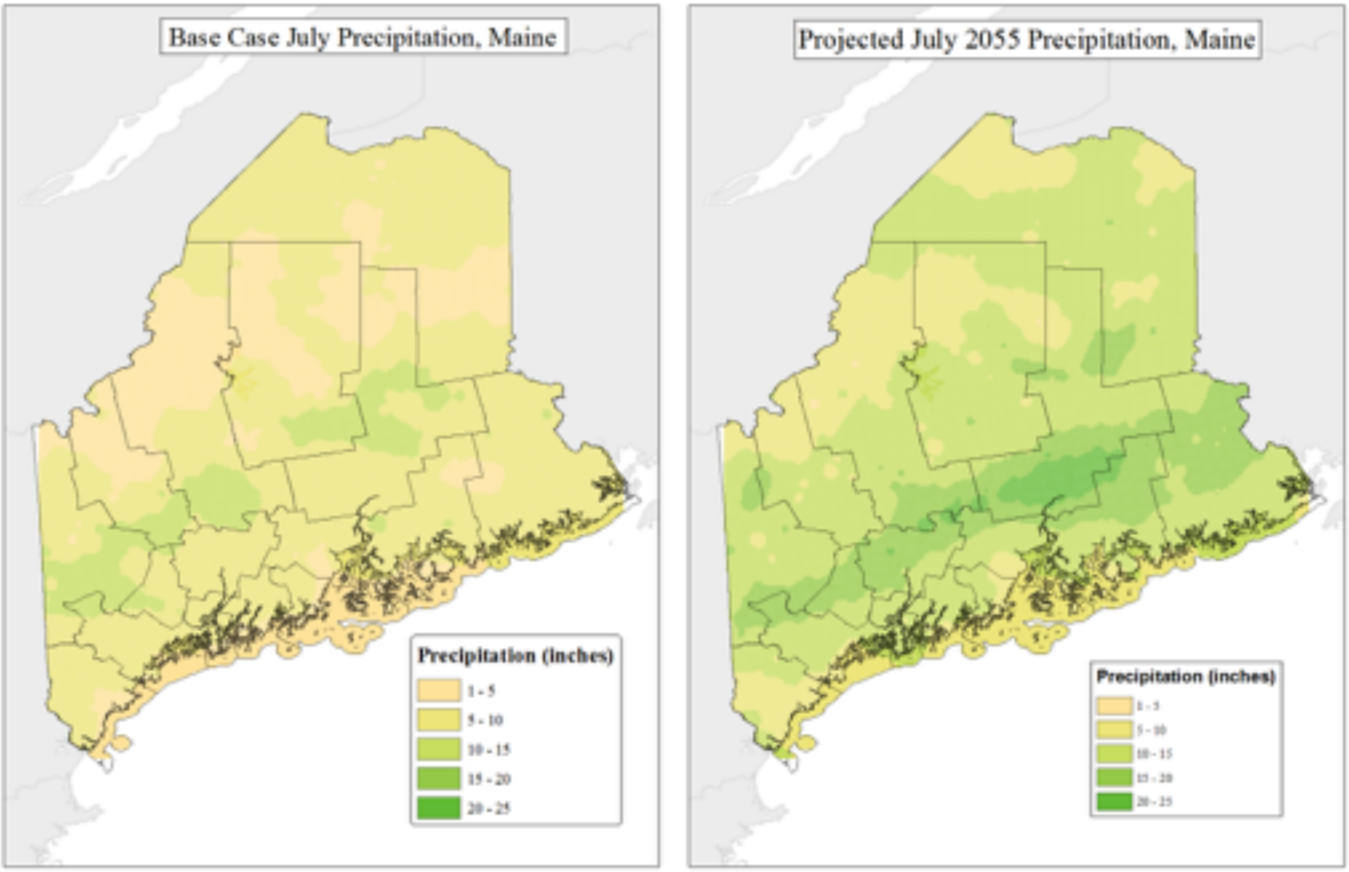

Figure 2. July projected base case and 2055 precipitation rates, based on WRF data dynamically downscaled from Community Earth System Model, Version 1.0 (CESM1) projections at 1 x 1.25 degree spatial resolution under RCP 8.5. The CESM simulation, output at 3-hourly intervals, is an ensemble member of the Coupled Model Intercomparison Project, Version 5 (CIMP5) (Gao et al., 2012). Base-case and 2050 precipitation rates were calculated for our simulation, and intermediate years were interpolated from these data.

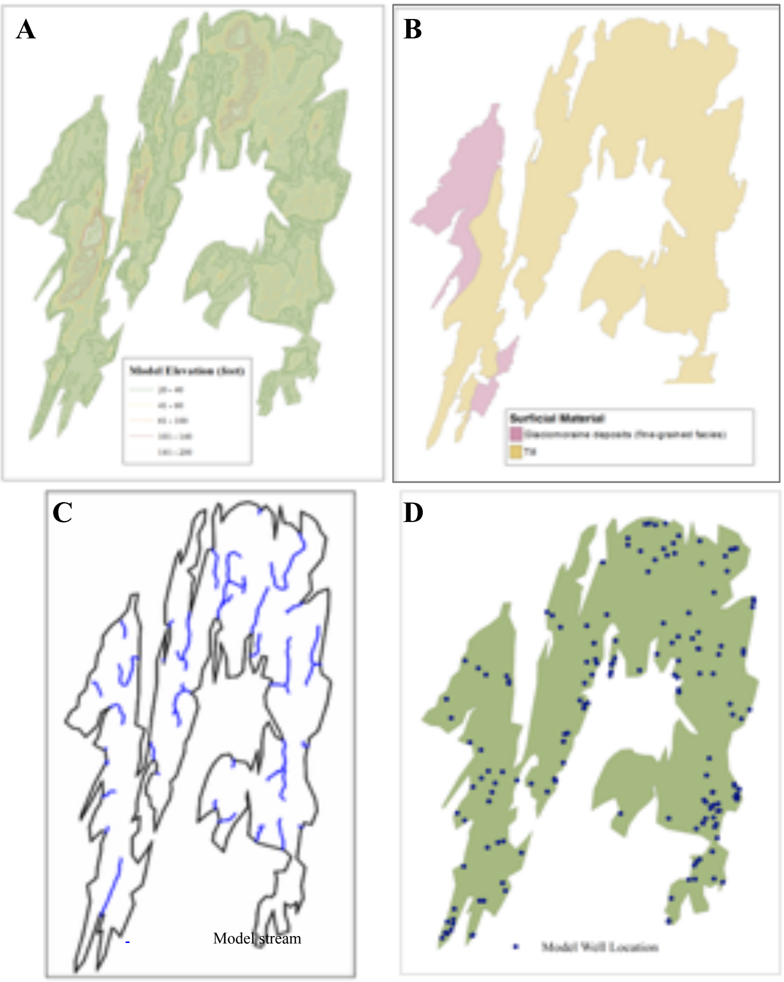

Figure 3. (A) Elevation contours of Sebascodegan Island interpolated to create model surface elevation. Elevation contours provided by the Maine Office of GIS. (B) Surficial material of Sebascodegan Island based on data provided by the Maine Office of GIS. Surficial materials consist of fine-grained glaciomoraine deposits